# Dropping balls through fluids, Milestone 5

Stephanie Merkler, Phuong Nguyen, James Woodhouse, Jatinder Kumar

December 9, 2005

**Drag is produced on a solid spherical body when it falls through a fluid. This semester, we are examining this phenomenon through modeling and experimentation. Topics that will be addressed are terminal velocity, interaction of the object with a surface, the effect of the properties of the fluid on the motion, and the effect of the container on the motion. A thorough literature review gives us the base for our model. In order to predict fall times, we account for the drag and buoyancy forces, the "added mass" phenomenon, and the "wall effect." We also optimize the fall time by incorporating the idea of terminal velocity into our model.**

## Introduction

As a sphere falls through a fluid, there are a number of forces acting on it. There is the obvious force of gravity that pulls the sphere down through the fluid. But there is also the force of drag that resists the falling of the sphere. The drag force through fluids such as oil and water is extremely substantial, however the significance of this force is not as great in a fluid such as air, and in most cases can be neglected. When a second fluid is introduced, there is another force acting on the ball during the transition from one fluid to the next. Also, when the size of the container is comparable to the size of the sphere, the effect of the container must be taken into

account. In order to create a model for a sphere falling through one or two fluids in different sized containers, the applicable forces must be summed and the resulting equations manipulated in order to allow us to make accurate predictions about the physical situation. This semester, our goal was to understand how the motion of a sphere is affected by all of these phenomena.

In this paper, we examine previous studies on various topics involving objects falling through fluids. We then develop the theory and governing equations involved in the modeling of each type of situation previously mentioned. Finally, we compare our model with experimental data in order to test the accuracy of our theory.

# Literature Review

In order to help us to better understand the ball dropping problem, we read the existing literature on the topic. This gave us a starting point on which to base our own model. We took various ideas and equations from the following authors in order to develop the theory that we use to model balls falling through fluids.

## Abaid, Adalsteinsson, *et.al.*

Abaid, Adalsteinsson, *et.al.* (*1*) explored the motion of falling spheres in strongly stratified fluids, in which their equilibrium density field varies with height. Similar to oceans or lakes, its fluid transitions are from low density at the top to high density at the bottom. Abaid, Adalsteinsson, *et.al.* document an internal "splash" phenomenon in which the falling sphere may reverse its direction of motion as it penetrates a region of strong density transition. Finally, they modeled this phenomenon including the levitation in the sphere with a nonlinear system of ordinary differential equations, which are shown in the theory portion of this paper.

This "levitation" phenomenon can be explained by turbulent mixing and entrainment surrounding the spheres, as well as the drag force exerted by the entrained fluid on the sphere.

These key physical mechanisms and behaviors of falling spheres through stratified fluids are hydrodynamically coupled between the sphere's body and ambient, stratified fluid. The findings of Abaid, Adalsteinsson, *et.al.* documented that the spheres produce an extraordinarily long transient time scale during their descent to the bottom layers.

The experiments that Abaid, Adalsteinsson, *et.al.* conducted involve using a glass tank of a specified dimension, distributed with salt in specific density profiles. An array of spherical glass beads are released from the top of the tank and the motion is recorded. The camera is positioned at a particular distance from the tank and height from the ground to the center of lens. This is extremely similar to the type of experiments that we will be conducting.

The nonlinear mathematical model from Abaid, Adalsteinsson, *et.al.* helps in the understanding of a falling ball through Newtonian fluids, such as water and oil. Consider the nonlinear dynamics associated with a fixed linear drag law moving through a monotonic, effective gravitational field,

$$m\frac{d^2}{dt^2}X + \alpha\frac{d}{dt}X = mg\left(\frac{\rho_b - \rho(X(t))}{\rho_b}\right). \tag{1}$$

$X(t)$ denotes the sphere's position as a function of time, initialized at the top of the tank. Abaid, Adalsteinsson, *et.al.* conducted experiments and verified that the density increases as a function of depth. Hence, in the case of the stratified density profile, $\rho(X)$ will be positive. The other variables, $m$ and $\rho_b$, denote the mass of the sphere and the density of the sphere respectively. The coefficient, $\alpha$, is the positive drag coefficient for the sphere, and lastly $g$ denotes the positive gravitational acceleration constant. By manipulating (1), we have

$$\frac{d}{dt}X|_{t=0} = v_{topterm} = mg\frac{\rho_b - \rho(0)}{\rho_b}, \tag{2}$$

which illustrates the minimum terminal velocity of the sphere. In order for the sphere's velocity, $\frac{dX}{dt}$, to achieve a local minimum, the derivative of the local velocity should vanish and the second derivative of the velocity should be positive at the minimum (*1*). To verify this argument, the

derivative of equation (1) is computed and evaluated at the minimum, giving

$$\frac{d^3}{dt^3}X = -g\frac{1}{\rho_b}\left(\frac{d}{dX}\rho(X)\frac{d}{dt}X\right) . \tag{3}$$

We need to account for another degree of freedom associated with the entrained fluid discussed above. The entrained fluid will be considered as the entrained mass of fluid itself moving with the sphere through the stratified fluid. This entrained fluid will viscously couple the sphere to the entrained fluid through the drag law by modifying the local sphere velocity with respect to both the sphere's motion and the local motion of the ambient fluid (*1*). This leads us to

$$m\frac{d^2}{dt^2}X - F\left(2\frac{d}{dt}X - \eta(t)\right) = mg\left(\frac{\rho_b - \rho(X(t))}{\rho_b}\right) , \tag{4}$$

$$\frac{d}{dt}\rho(t) = \beta(\rho(X(t)) - \rho(t)) , \tag{5}$$

which illustrate the effect of the entrained, ambient fluid by replacing a point with mass $z$, which is located at a fixed distance $\omega$, above the sphere with velocity $\eta(t)$, and density $\rho(t)$. These equations also include the final result of the hydrodynamically coupling as a new degree of freedom, in order to account for the falling sphere by the drag law. The relative speed of the body is compared with its fluid surroundings. This simply means that the entrained fluid can be thought of as a spherical object which occupies the space of an actual sphere and has its own mass, velocity, and density. By observing these equations, one can see the self-consistent internal "splash" experienced by the sphere. The force balance between the viscous drag force relative to the falling sphere and the buoyancy force is given by

$$z\frac{d}{dt}\eta(t) - F\left(\eta(t) - \frac{d}{dt}X\right) = zg\left(\frac{\rho(X(t) - \omega) - \rho(t)}{\rho(t)}\right) . \tag{6}$$

This determines the self-consistency of the dynamics of the point of mass. The idealized fluid particle will be able to develop negative buoyancy that results in a "plume" phenomenon which is consistent with the model above.

## Richardson

We also read a paper by Richardson (*2*). Part I of Richardson's experiment looks into the study of the motion of a solid sphere as it strikes a liquid surface vertically, the evolution of the cavity formation, and the shape of the cavity formed. The shape of the air cavity formed is further investigated and explained in terms of pressure and the resistance to motion in the cavity. Part II looks into the study of the impact forces consisting of theoretical aspects of impact on liquids, and the calculation on the impact forces.

In order to study the flow of water in detail as the sphere passes vertically downward through the cavity, a series of fine air bubbles was produced beneath it. The upward speed of the bubbles was very small compared to the downward speed of the projectile. The potential, or amount of energy stored, due to a source may in fact be added to that of a uniform stream to give that at any point $(r, \theta)$, with $r$ measured from the source and $\theta$ from the zenith,

$$\frac{\phi}{V} = \frac{a^2}{r - r\ \cos(\theta)}\,, \tag{7}$$

hence the streamline

$$\frac{\psi}{V} = a^2 \cos(\theta) - \frac{1}{2} r^2 \sin^2(\theta)\,. \tag{8}$$

The streamline, which is a line that is tangent to the velocity vector at a given instance, divides to pass the obstacle and is given by

$$a^2 = a^2 \cos(\theta) - \frac{1}{2} r^2 \sin^2(\theta)\,. \tag{9}$$

Simplification give us,

$$r = a\ \csc\left(\frac{\theta}{2}\right)\,, \tag{10}$$

so that the source cannot be set to make the dividing line conform to a sphere of radius $a$. The corresponding stream function for a point distance $r$ from the source and $c$ from the upper end

of the sink is

$$\frac{\psi}{V} = a^2 cos(\theta) - \frac{1}{2} r^2 sin^2(\theta) - a(r - c)\,. \tag{11}$$

It appears that $\theta$ is independent of density. The piling up of surface water at first impact, causes faster closing of the lid of the cavity but, being evanescent, has little effect on the closure at depth. The speed of the sphere shot into the water does not have an effect on the shape of the cavity formed.

An attempt has been made to measure the air pressure developed in the cavity during the underwater trajectory, since such information may help to elucidate the mechanism of cavity closure and disintegration. It is not to be expected that the pressure will deviate much from the atmospheric or the local hydrostatic value, so a sensitive recorder is necessary.

Resistance in the cavity is plotted by a displacement-time curve of the projectile after it has formed a cavity. At the entry speeds involved, the frictional resistance was the paramount force causing deceleration. If $M$ is the mass of the projectile, $d$ its diameter, $V$ its speed, $\rho$ the density of the liquid,

$$M\frac{\partial V}{\partial t} = Mg - C_d \left(\frac{\pi d^2}{4}\right) \left(\frac{1}{2}\rho V^2\right)\,, \tag{12}$$

where $C_d$ is a drag coefficient which relates the frictional force to the projected area of the projectile and the pressure at its front stagnation point in the conventional fashion.

This may be written, when $c$ is the specific gravity of the solid in terms of the liquid and $s$ the path traced by the sphere as

$$\frac{1}{6}\pi d^3 c \left(g - V\frac{\partial V}{\partial s}\right) = C_d \pi d^2 \left(\frac{V^2}{8}\right)\,. \tag{13}$$

When the speed and deceleration are such that the effect of gravity can be neglected, we have for the drag coefficient

$$C_d = 3.05 \left(d\frac{c}{s}\right) log \left(\frac{Vc}{V}\right), \tag{14}$$

$V_o$ and $V$ being the speeds at the two ends of the track $s$. The motion of the projectile after entry appears to be unaffected by air pressure. A number of attempts have been made to calculate theoretically the drag coefficient of a sphere in a cavity. However, the specific gravity of the solid and the compressibility of gas and liquid have no great effect on the coefficient $C_d$. Experiments made with spheres of different diameters at different speeds will experience the same forces and have identical cavity forms at corresponding times if the Froude number is the same.

There are two theoretical aspects from which one can regard the impact on liquids, both based on the idea of the "added mass" of liquid which the body sets in motion. Using the older theory, it is supposed that when a body of mass $M$ enters a liquid, there is a sudden reduction of its velocity which is ascribed to an apparent addition to its mass by the mass of liquid $m$ set instantaneously in motion. Thus if $V_o$ is the velocity just before impact, $V_1$ just after,

$$MV_o = (M+m)V_1. \tag{15}$$

If an axially symmetrical body hits a liquid at a speed $V_o$, the force at any subsequent instant is given by

$$F = -M\frac{\partial V}{\partial t} = \frac{\partial}{\partial t}(mV) = \frac{\partial}{\partial t}\left(\frac{2}{3}\pi c^3\rho V\right) = \frac{2}{3}\pi c^3\rho\frac{\partial V}{\partial t} + 2\pi c^3\rho V^2\frac{\partial c}{\partial h}\,, \tag{16}$$

where $h$ is the depth of the immersion and $c$ is the radius of the wetted perimeter. For a sphere,

$$h = a - \sqrt{a^2 - c^2}\,, \tag{17}$$

$$\frac{\partial c}{\partial h} = \frac{c}{\sqrt{a^2 - c^2}}\,, \tag{18}$$

so

$$F = -\frac{mF}{M} + 2\pi c\sqrt{a^2 - c^2}\rho V^2. \tag{19}$$

The maximum value of this occurs when $m = \frac{1}{2}M$ and is then $0.86c^2\tan(\gamma)$.

## Renganathan, Turton, and Clark

In 1989, Renganathan, Turton, and Clark (*3*) developed equations of motion for spherical particles moving vertically in an infinite fluid. They assumed that the drag coefficient on the particles during this unsteady state motion was similar to that of steady state motion. They restricted their analysis to dense objects falling in less dense fluids, which allowed them to ignore the effects of acceleration of the fluid surrounding the object and still obtain accurate results. From their theory, they were able to predict the distance it took for an object to reach 90% of its terminal velocity while falling vertically downward in fluid. They also found a correlation equation that predicts the distance traveled as a function of the drag coefficient at terminal velocity.

It has been found through an experiment by Turton and Levenspiel (*4*) that for spherical particles,

$$C_{Dt} = \frac{24}{Re_t}(1 + 0.173Re_t^{0.657}) + \frac{0.413}{1 + 16300Re_t^{-1.09}} \ , \tag{20}$$

where $C_{Dt}$ is the drag coefficient at the terminal velocity of the particle and $Re_t$ is the Reynolds number at terminal velocity. This is given by $Re_t = \frac{\rho u_t D_p}{\mu}$, where $\rho$ is density of the particle, $u_t$ is the terminal velocity, $D_p$ is the characteristic length of the particle $p$, and $\mu$ is the viscosity of the fluid.

From the analysis by Renganathan, Turton, and Clark (*3*), consider a spherical particle with diameter $d_p$, density $\rho_s$, mass $m_s$, and volume $V_s$ dropped into a fluid of density $\rho$ and viscosity $\mu$. Let $u$ be the velocity and $a$ be the acceleration of the particle at any time $t$. The equation of motion for the particle is

$$m_s a = V_s(\rho_s - \rho)g - \frac{\pi d_p^2}{4} C_D \frac{\rho u^2}{2} \ . \tag{21}$$

Renganathan, Turton, and Clark were able to find a differential equation relating distance traveled to the drag coefficient,

$$\frac{dX}{dY} = \frac{4Y}{3[C_{Dt} - Y^2 f(Re_t Y)]} \ , \tag{22}$$

where $X = x\gamma/d_p$ ($x$ is the displacement of the particle and $\gamma = \rho/\rho_s$), $Y = Re/Re_t$, and $f$ is some function such that $C_{Dt} = f(Re_t)$. Here, we assume that the drag coefficient $C_D$ obeys the same function as the drag coefficient at terminal velocity $C_{Dt}$ does, thus $C_D = f(YRe_t)$. If equation (20) is used as $f$, when equation (22) is solved numerically, we have an equation that predicts the distance traveled by a spherical particle as a function of the drag coefficient at terminal velocity. Renganathan, Turton, and Clark found that this solution predicted values that compared well with experimental data.

## White

For a general background in fluids, we looked at Fluid Mechanics by Frank M. White (*5*). White gives an extensive introduction to fluid mechanics. The chapter on "Flow Past Emersed Bodies" gives characterizations of the various types of flows. These flows include Laminar, Transient, and Turbulent. Each one has different governing equations for drag which may become useful in our modeling.

White (*5*) describes the drag coefficient by

$$C_D = \frac{F_{drag}}{\frac{1}{2}\rho V^2 A}\,. \tag{23}$$

The area $A$ is one of three types:

- $Frontal\ area$: used for thick, stubby bodies, such as spheres, cylinders, cars, missiles, projectiles, and torpedoes.
- $Planform\ area$: the body area seen from above, used for wide, flat bodies such as wings and hydrofoils.
- $Wetted\ area$: used for ships and barges.

The formula White gives us for drag on simple, three-dimensional bodies (i.e. a sphere) is written as

$$C_D = \frac{24}{Re_d}\,, \tag{24}$$

where $Re_d$ is the Reynolds number, a dimensionless parameter given by

$$Re_d = \frac{\rho U d}{\mu}\,. \tag{25}$$

Equation (24) works well when $Re_d \leq 1$.

For an ellipsoid with an $L/d$ of 1 ($L = d$ which is a sphere), $C_D$ is $.47$ for Laminar flow and $.2$ for Turbulent flow (*5*).

## Jenny *et.al.*

Jenny $et.\ al.$ (*6*) (*7*) studied the effect of a sphere falling or ascending under gravitational influence in a Newtonian fluid. They also investigated the scenario of transition to chaos regimes exhibited on a sphere. These investigations were done by numerical simulation. The mathematical formulation developed is parameterized using two dimensionless parameters. The first is the solid and fluid density ratio and the second is the generalized Galileo number, which expresses the ratio between the gravity-buoyancy and viscosity effects. They also documented that for all density ratios, the vertical fall or ascension becomes unstable via a regular axisymmetry breaking bifurcation. In a dynamic system, a bifurcation is a period doubling, quadrupling, *etc.* that accompanies the onset of chaos. It was noted that this bifurcation sets in slightly earlier for lighter spheres than for dense ones. A change is found in its trajectory from a steady oblique fall or ascension to an oscillating oblique movement. The initiation of this transition occurs prior to its loss of stability.

The transition scenario of spherical particles moving freely are under the influence of gravity, buoyancy and hydrodynamic forces. The breaking of axisymmetry is influenced by the

additional degrees of freedom of the particle and the dependency on two dimensionless parameters which characterize the parameter space. It was noted earlier that these two parameters are the density ratio of the sphere and fluid, and the Galileo number with the ratio of gravity-buoyancy and viscosity effects all incorporated. These mathematical relationships are shown below, which will give a first step to the development of the formulation for this physical phenomenon.

We have

$$G = \frac{\sqrt{\left|\frac{\rho_0}{\rho} - 1\right| gd^3}}{\nu}\,, \tag{26}$$

where $g$ is the acceleration constant due to gravity, $d$ is the sphere diameter, and $\nu$ is the kinematic viscosity of the fluid. In axisymmetric (laminar) regimes, numerical simulations established the empirical laws provided by the drag coefficient $C_D$ as a function of the Reynolds number,

$$C_D(Re_\infty) = \frac{4G^2}{3Re_\infty^2}\,. \tag{27}$$

This yields an easy conversion between the asymptotic Reynolds number, $Re_\infty$ and the Galileo number. This problem of a freely moving solid object through fluid contains six degrees of freedom. The degrees of freedom are the velocity of the center of mass $u$, and the angular velocity of rotation around the center of mass, denoted $\Omega$. The resulting physical system is made up of two coupled phases, fluid and the solid sphere. The fluid, or the flow field, can be described by the fluid velocity $\nu$ and the pressure $p$ which is perturbed by the motion of the particle. This fluid phase is characterized by its density $\rho$ and the kinematic viscosity $\nu$. As for the solid sphere, its motion is set in by buoyancy and gravity forces and the action of the fluid perturbs its trajectories. This phase is characterized by its density $\rho_0$ and its diameter $d$.

The Navier-Stokes relation,

$$\frac{\partial \nu}{\partial t} + [(\nu - u)\cdot \bigtriangledown]\nu = -\bigtriangledown \cdot p + \frac{1}{G}\bigtriangledown^2 \cdot \nu\,, \tag{28}$$

$$\bigtriangledown \cdot \nu = 0\,, \tag{29}$$

describes the fluid field. The complete boundary condition (non-slip) on the sphere surface $S$ is illustrated by

$$\nu = u + \Omega \times r \tag{30}$$

where $r_s$ represents for the position vector on the sphere surface.

This procedure involves numerical simulation of the coupling between the Navier-Stokes relations and the motion equations, which includes the necessity of using an implicit time discretization.

# Theory

## One-fluid model

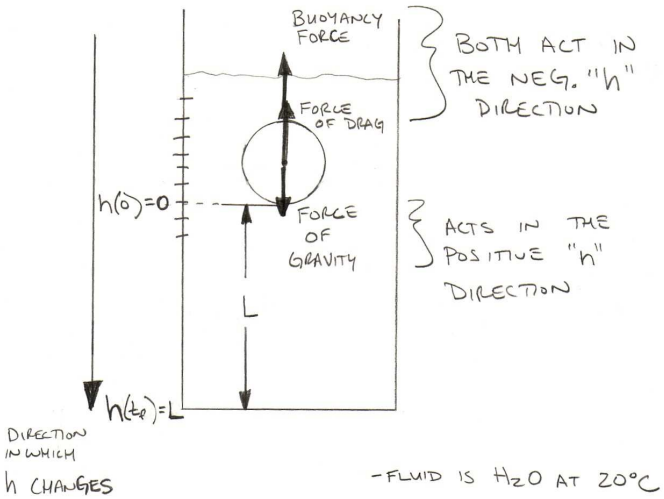


Figure 1: Ball falling through a single fluid.

In order to establish the theoretical model for a ball falling through a single fluid (Figure 1),

we first sum the buoyancy and drag forces acting on the ball:

$$F_{drag} = -\frac{1}{2} C_D \rho_l A h'^2 \ , \tag{31}$$

$$F_{buoyancy} = (\rho_m - \rho_l) V g \ , \tag{32}$$

where $C_D$ is the coefficient of drag, $A$ is the cross sectional area of the ball, $h$ is the height of the ball as a function of time $t$, $\rho_l$ is the density of the fluid (in our case, water), $\rho_m$ is the density of the ball, $V$ is the volume of the ball, and $g$ is the acceleration due to gravity (for our experiments, $g$ is assumed to be equal to $9.81\ m/s$). Note that in (31), the force of drag is proportional to the square of the velocity of the ball $h'$. Applying Newton's law (sum of the forces = mass $\times$ acceleration), we sum (31) and (32) and set this equal to $mh''$, where $m$ is the mass of the ball and $h''$ is the acceleration, giving us our complete model:

$$mh'' = -\frac{1}{2} C_D \rho_l A h'^2 + (\rho_m - \rho_l) V g \ . \tag{33}$$

Next, we nondimensionalize this model. To do this, we scale both the time $t$ and the height $h$. We set $H = \frac{h}{L}$, where $L$ is the total height of the fall, and $T = \frac{t}{\tau}$, where $\tau$ is a reasonable time scale that we will determine later. After finding $h'$ and $h''$ according to this scaling, we replace them in (33) and are left with

$$m \left( \frac{L}{\tau^2} \right) \frac{d^2 H}{dT^2} = -\frac{1}{2} C_D \rho_l A \left( \frac{L}{\tau} \frac{dH}{dT} \right)^2 + (\rho_m - \rho_l) V g \ . \tag{34}$$

This can easily be simplified by dividing both sides by $\frac{L}{\tau^2}$, solving for a reasonable $\tau$ ($\tau = \sqrt{\frac{mL}{(\rho_m - \rho_l) V g}}$), and combining the constants into one nondimensional constant $\varepsilon$,

$$H'' = -\varepsilon H'^2 + 1 \ , \tag{35}$$

$$\varepsilon = \frac{1}{2} \frac{C_D \rho_l A L}{m} \ . \tag{36}$$

Since the initial nondimensional height $H = 0$ and the initial velocity of the ball $H^{'} = 0$, we have the initial conditions

$$H(0) = 0,\ H^{'}(0) = 0. \tag{37}$$

$\varepsilon$ is a good parameter to use because it relates the coefficient of drag, which is initially unknown in our experiment, to the physical properties of the ball, which will be varied in our experiment.

We also know that the final nondimensional height will be equal to $1$, so we have

$$H(T_f) = 1. \tag{38}$$

## Two-fluid model

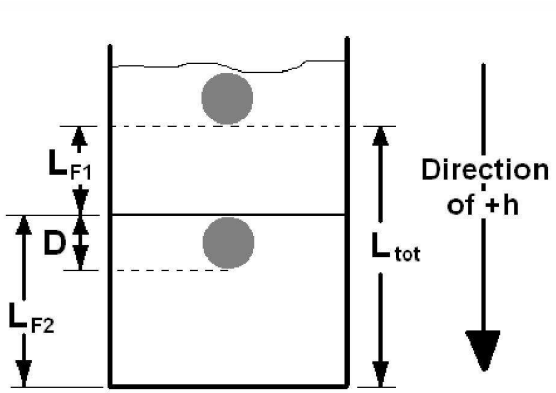


Figure 2: Ball falling through two fluids.

Next, we develop a model for a sphere falling through two different fluids (Figure 2). We divide the column of fluid into three regions. Region 1 contains Fluid 1 and only has the physical properties of Fluid 1. It has length $L_{F1}$, and the height of the ball in this region is given by $h_1$. Region 2 is the interface having length $D$, the diameter of the sphere. It accounts for the physical properties of both Fluid 1 and Fluid 2. The height of the ball in this region is given by $h_2$. Lastly, Region 3 contains Fluid 2, has only the physical properties of Fluid 2, and

has length $L_{F2}$. The height of the ball in this region is given by $h_3$. As the sphere falls through Region 1, the theoretical model for Region 1 is "on". When the sphere reaches the height of $L_{F1}$, the equation for Region 1 is turned "off" and the model for Region 2 is enabled. It is then immediately disabled when the sphere reaches $L_{F1} + D$. This then activates the last model for Region 3.

For Region 1 and Region 3, we use the one-fluid model, as given above. However, for Region 2, the theory must be modified. The sphere will have an impact once it makes its transition from Fluid 1 to Fluid 2. This impact is based on the idea of the "added masses" of fluid which the body sets in motion. According to Richardson (*2*), when a body of mass $m$ enters a liquid there is a sudden reduction of its velocity which is attributed to an apparent addition to its mass by the mass of Fluid 1 set instantaneously in motion. The following equation describes this added mass theory:

$$(mh_i^{'})^{'} = \frac{2}{3}\pi c^3 h_i^{''} + 2\pi c^2 \rho_1 h_i^{'2} \frac{\partial c}{\partial h_i}\,, \tag{39}$$

where $h_i$ is the depth of immersion in Region 2, $c$ is the radius of the wetted perimeter, and $\rho_1$ is the density of Fluid 1. The wetted perimeter is the area of the ball that is covered by Fluid 2. Richardson gives the relationship of $h_i$ and $c$ as follows:

$$h_i = D - \sqrt{(D^2 - c^2)} \tag{40}$$

where $D$ is the diameter of the ball. This equation comes from the geometrical relationship between $h_i$ and $c$, the height of immersion at the interface and the diameter of the wetted perimeter, respectively. These variables change as the sphere passes through the interface layer. The relationship is simply the difference between the diameter of the sphere, $D$, and the distance that the sphere travels through the interface layer, $\sqrt{(D^2 - c^2)}$. From this relationship, we can solve for $c$ in terms of $h_i$ and take the derivative,

$$c = \sqrt{-h_i(h_i - 2D)}\,, \tag{41}$$

$$\frac{\partial c}{\partial h_i} = -\frac{h_i - D}{\sqrt{-h_i(h_i - 2D)}}\,. \tag{42}$$

The final step of this derivation is to determine $h_i$ in terms of $h_2$ and $L_{F_1}$, the total height that the sphere has traveled and the length of Fluid 1. We know that when $h_i = 0$, $h_2 = L_{F_1}$ because the ball has just traveled through the length of Fluid 1. Also, when $h_i = D$, $h_2 = L_{F_1} + D$. This gives us

$$h_i = h_2 - L_{F_1}\,, \tag{43}$$

which gives us

$$c = \sqrt{D^2 - h_2^2 - L_{F1}}\,, \tag{44}$$

$$\frac{\partial c}{\partial h_2} = \frac{-(D - h_2 - L_{F1})}{\sqrt{2D(h_2 - L_{F1}) - h_2 - L_{F1}}}\,. \tag{45}$$

As before, we must also take into account the force of drag and the buoyancy force on the ball,

$$F_{drag} = -\frac{1}{2} C_{D_1} \rho_1 A h_2'^2\,, \tag{46}$$

$$F_{buoyancy} = (\rho_m - \rho_2) V g\,, \tag{47}$$

where $C_{D_1}$ is the coefficient of drag in Fluid 1, $A$ is the cross sectional area of the ball, $\rho_1$ is the density of Fluid 1, $\rho_2$ is the density of Fluid 2, $\rho_m$ is the density of the ball, $V$ is the volume of the ball, and $g$ is the acceleration due to gravity. Note that at the interface, the added mass of Fluid 1 with density $\rho_1$ surrounds the sphere once it transfers to Fluid 2. Only $\rho_2$ appears in the buoyancy term because it has the physical force that opposes the ball falling and pushes the sphere upwards.

Now, the equation of motion for Region 2 is

$$m h_2'' = -\frac{2\pi}{3} \rho_1 h_2'' c^3 - \left( \frac{2\pi}{3} c^2 \rho_1 \frac{\partial c}{\partial h_2} - \frac{\rho_1 C_{D_1} A}{2} \right) h_2'^2 + (\rho_m - \rho_2) V g\,, \tag{48}$$

where

$$c = \sqrt{D^2 - h_2^2 - L_{F1}}\,, \tag{49}$$

$$\frac{\partial c}{\partial h_2} = \frac{-(D - h_2 - L_{F1})}{\sqrt{2D(h_2 - L_{F1}) - h_2 - L_{F1}}} \,. \tag{50}$$

At time $t_1$, the ball has reached the interface of the fluids, so $h_2$ is $L_{F_1}$. At this time, the velocity $h_2^{'}(t_1)$ is the same as the velocity is equal to the final velocity in Region 1, $h_1^{'}(t_1)$. This gives the following initial conditions:

$$h_2(t_1) = L_{F_1} \,, \tag{51a}$$

$$h_2^{'}(t_1) = h_1^{'}(t_1) \,. \tag{51b}$$

At time $t_2$, the ball has reached the bottom of Region 2, which gives us

$$h_2(t_2) = L_{F_1} + D \,. \tag{52}$$

The theory for the regions in Fluids 1 and 2 is the same as the original one-fluid model with a few changes due to the difference in physical properties of the fluids, such as densities and coefficient of drag $C_D$. In Region 1, we have

$$m h_1^{''} = -\frac{\rho_1 C_{D_1} A h_1^{'2}}{2} + (\rho_m - \rho_1) V g \,, \tag{53a}$$

$$h_1(0) = 0 \,, \tag{53b}$$

$$h_1^{'}(0) = 0 \,, \tag{53c}$$

$$h_1(t_1) = L_{F_1} \,. \tag{53d}$$

The initial conditions come from the fact that at time $t = 0$, the ball is at the zero height, and begins with zero velocity. At time $t_1$, the ball has reached the end of the length of Region 1, $L_{F_1}$.

Similarly, in Region 3, we have

$$mh_3^{''} = -\frac{\rho_2 C_{D_2} A h_3^{'2}}{2} + (\rho_m - \rho_2)Vg\,, \tag{54a}$$

$$h_3(t_2) = L_{F_1} + D\,, \tag{54b}$$

$$h_3^{'}(t_2) = h_2^{'}(t_2)\,, \tag{54c}$$

$$h_3(t_3) = L_{tot}\,. \tag{54d}$$

As stated before, at time $t_2$, the ball has reached the bottom of Region 2, giving the initial condition (54b). Like before, the initial velocity in Region 3, $h_3^{'}(t_2)$, is the same as the final velocity in Region 2, $h_2^{'}(t_2)$, giving us (54c). At time $t_3$, the ball has reached the bottom of Region 3, and has traveled the entire length of the fall $L_{tot}$, giving us (54d).

We now have our complete dimensional model for the motion of the ball through Fluid 1, the interface of the fluids, and Fluid 2. Next, we nondimensionalize the model using the following scaling:

$$H_1 = \frac{h_1}{L_{tot}},\ H_2 = \frac{h_2}{L_{tot}},\ H_3 = \frac{h_3}{L_{tot}},\ T = \frac{t}{\tau} \tag{55}$$

where

$$\tau = \frac{\sqrt{mL_{tot}}}{\sqrt{(\rho_m - \rho_1)Vg}}\,. \tag{56}$$

By applying this scaling to (48-54d), we arrive at the following nondimensionalized model:

Region 1:

$$H_1^{''} = -\varepsilon H_1^{'2} + 1\,, \tag{57a}$$

$$H_1(0) = 0\,, \tag{57b}$$

$$H_1^{'}(0) = 0\,, \tag{57c}$$

$$H_1(T_1) = \frac{L_{F_1}}{L_{tot}}\,. \tag{57d}$$

Region 2:

$$H_2^{''} = -\beta C^3 H_2^{''} + \delta + \varepsilon H_2^{'2} - \beta C^2 G(H_2) H_2^{'2}\,, \tag{58a}$$

$$H_2(T_1) = \frac{L_{F_1}}{L_{tot}}\,, \tag{58b}$$

$$H_2^{'}(T_1) = H_1^{'}(T_1)\,, \tag{58c}$$

$$H_2(T_2) = \frac{L_{F_1} + D}{L_{tot}}\,. \tag{58d}$$

Region 3:

$$H_3^{''} = -\zeta H_3^{'2} + \delta\,, \tag{59a}$$

$$H_3(T_2) = \frac{L_{F_1} + D}{L_{tot}}\,, \tag{59b}$$

$$H_3^{'}(T_2) = H_2^{'}(T_2)\,, \tag{59c}$$

$$H_3(T_3) = 1\,. \tag{59d}$$

where

$$\varepsilon = \frac{\rho_1 C_{D_1} A L_{tot}}{2m}\,, \tag{60a}$$

$$\zeta = \frac{\rho_2 C_{D_2} A L_{tot}}{2m}\,, \tag{60b}$$

$$\beta = \frac{2\pi}{3}\frac{\rho_1 L_{tot}^3}{m}\,, \tag{60c}$$

$$C = \frac{c}{L_{tot}}\,, \tag{60d}$$

$$\delta = \frac{\rho_m - \rho_2}{\rho_m - \rho_1}\,, \tag{60e}$$

$$G(H_2) = -\frac{H_2 - \frac{L_{F1}}{L_{tot}} - \frac{D}{L_{tot}}}{\sqrt{\frac{2D(H_2 - \frac{L_{F1}}{L_{tot}})}{L_{tot}^2} - \left(H_2 - \frac{L_{F1}}{L_{tot}}\right)^2}}\,. \tag{60f}$$

Region 1 and 3 have an exact solution that can be calculated with relative ease. By letting $v = H^{'}$ in Region 1, (57a) becomes

$$v^{'} = -\varepsilon v^2 + 1\,. \tag{61}$$

We divide both sides by $1 - \varepsilon v^2$ and integrate to get

$$\frac{1}{\sqrt{\varepsilon}} \tanh^{-1}\left(\sqrt{\varepsilon} v\right) = T + C_0 \,. \tag{62}$$

Solving this solution for $v$ and plugging $H^{'} = v$ back into the equation gives

$$H^{'} = \frac{1}{\sqrt{\varepsilon}} \tanh\left(\sqrt{\varepsilon}(T + C_0)\right) \,. \tag{63}$$

Integrating, plugging in all initial conditions and solving from zero to the desired time gives the exact solution

$$H(t) = \frac{1}{\sqrt{\varepsilon}} \int \tanh\left(\sqrt{\varepsilon} T\right) . \tag{64}$$

Similarly, the solution for Region 3 is

$$H(t) = \frac{1}{\sqrt{\zeta}} \int \tanh\left(\sqrt{\zeta} T\right) . \tag{65}$$

Region 2 cannot easily be solved analytically and must be solved numerically.

The general process for numerically solving these equations is as follows, using the MATLAB code found in Appendix A. For Region 1, we numerically solve (57a) using the initial conditions (57b) and (57c). Since the coefficient of drag $C_{D_1}$ for Fluid 1 is unknown, we use the bisection method to find the $\varepsilon$ that allows us to obtain the value (57d), which is found from data from our experiment. This then allows us to solve for $C_{D_1}$ to use for future predictions. We then find initial condition (58c) by taking the derivative of the solution to (57a). Initial condition (58b) is found from data from the experiment. Since all other constants in (58a) are known from the experiment, we solve this ODE numerically. We check the accuracy of this solution with the value (58d) from our data. Again, we take the derivative of this solution to find initial condition (59c). Using our data to find the constants in (59a) and initial condition (59b), we solve the ODE and match the solution with the value (59d).

Note that when Fluid 1 is air, we assume that the coefficient of drag in air is very small, which allows us to assume that $\varepsilon = 0$. This allows us to skip the step of finding the proper $\varepsilon$ to fit our data.

## Wall effect

In this section, we will focus on the model for a sphere falling through water, where the radius of the sphere is comparable to that of the container. In order to correct the wall effect induced by the size of the container, Faxen's formula can be applied (*8*). First, consider a hard sphere with radius $a$ (or $D/2$ where $D$ is the diameter of the sphere) moving with velocity $U$ in an unbounded quiescent fluid with viscosity $\eta$. The sphere experiences a hydrodynamic drag force opposite to its direction of motion. If there is no slip at the boundary between the hard sphere and fluid, the drag force is given by Stokes regime,

$$F_d = -6\pi\eta a U \,. \tag{66}$$

The diffusion coefficient $D$ of the sphere is then given by the Stokes-Einstein relation,

$$D = \frac{k_B T}{6\pi\eta a} \,, \tag{67}$$

where $k_B$ is the Boltzmann constant and $T$ is the temperature of the system. When the sphere is close to a flat wall or is confined between two flat walls, the drag force increases and its diffusion is hindered. Because of the linearity of the Stokes equations, the drag force can be separated into independent components for motion parallel and perpendicular to the wall. We will focus only on the parallel component because the motion of the sphere is parallel to the wall. For the parallel component of the wall-drag force, we multiply the drag force in an unbounded liquid by $\lambda_{\|}$, which gives us

$$F_{\|} = -6\pi\eta a U \lambda_{\|} = F_d \lambda_{\|} \,. \tag{68}$$

The correction factor is simply obtained by utilizing the diffusion coefficient for parallel motion of the sphere relative to the wall,

$$D_{\|} = \frac{k_B T}{6\pi\eta\lambda_{\|} a} = {\lambda_{\|}}^{-1} D \,. \tag{69}$$

The exact solution for the wall-drag force does not have a closed analytical form and it is difficult to solve. Therefore, the most commonly used representation of $\lambda_{\parallel}$ is usually an approximation utilizing the so-called "method of reflections." (9) The method of reflections is an iterative series solution technique that decomposes the velocity and the pressure fields into a linear superposition of terms of successively higher order in the number of wall and sphere boundary interactions. This method assumes that the motion of a sphere near a wall induces a pressure and velocity distribution in the adjacent fluid. The terms in the expansion are constrained to the boundary conditions on the sphere and the confining walls. Therefore, the solutions for $\lambda_{\parallel}$ obtained with this method are usually expressed as a power series in $a/R$, where R is the radius of the cylinder, or the distance from the center of the sphere to the wall of the container. This method gives us the Faxen's correction factor for the drag force due to two walls and in a cylindrical tube, ${\lambda_{\parallel}}^{I}$ and ${\lambda_{\parallel}}^{II}$, respectively,

$$ {\lambda_{\parallel}}^{I} = \left[1 - 1.004\left(\frac{a}{R}\right) + 0.418\left(\frac{a}{R}\right)^3 + 0.21\left(\frac{a}{R}\right)^4 - 0.169\left(\frac{a}{R}\right)^5 + ...\right]^{-1}, \tag{70a} $$

$$ {\lambda_{\parallel}}^{II} = \left[1 - 2.10444\left(\frac{a}{R}\right) + 2.08877\left(\frac{a}{R}\right)^3 - 0.94813\left(\frac{a}{R}\right)^5 - 1.372\left(\frac{a}{R}\right)^8 - 4.19\left(\frac{a}{R}\right)^{10} + ...\right]^{-1}. \tag{70b} $$

For simplicity, we will use $K_w$ as a universal notation for the Faxen's wall correction factor. We will use the proper correction factor (${\lambda_{\parallel}}^{I}$ or ${\lambda_{\parallel}}^{II}$) for $K_w$, depending on the physical situation.

When used in solving the one-fluid model, the correction factor $K_w$ is multiplied onto the equation for $\varepsilon$, giving

$$ \varepsilon = \frac{1}{2}\frac{C_D \rho_l A L K_w}{m} . \tag{71} $$

The ODE is then solved as before.

## Optimization of fall time

The goal of this section is to find the drop height that allows the ball to have the fastest fall time in the two-fluid set-up. We want to choose a drop height above the interface of the two fluids

such that the time to fall of the sphere is optimized. The idea behind this theory involves the notion that the sphere should enter the second fluid at its terminal velocity in this fluid, rather then any faster, so that any additional velocity that the sphere may have at this point does not go to waste. Also, if the sphere enters the second fluid traveling at its terminal velocity rather then a lower velocity, it will take no more time for it to accelerate, and therefore will travel the fastest through the second fluid. So, we determine the terminal velocity $v_t$ of the sphere through the second fluid and use it to determine what height to drop the sphere from so that it reaches $v_t$ just as it begins to enter the second fluid.

To determine $v_t$, we first examine the nondimensional equation from the one-fluid model,

$$H_1^{''} = -\varepsilon H_1^{'2} + 1\,. \tag{72}$$

We know that when the sphere reaches $v_t$, the acceleration term $H^{''}$ is zero. Setting the right-hand side equal to zero and solving for $H^{'}$ in terms of $\varepsilon$ will give us the nondimensional terminal velocity,

$$H_{terminal}^{'} = \frac{1}{\sqrt{\varepsilon}}\,, \tag{73}$$

where

$$\varepsilon = \frac{\rho_{water} C_{D_{water}} A L_{tot}}{2m}\,. \tag{74}$$

Now we scale this nondimensional terminal velocity by the scaling factor $\frac{L_{tot}}{\tau}$, giving us the dimensional terminal velocity,

$$v_t = \sqrt{\frac{2(\rho_m - \rho_{water})Vg}{\rho_{water} C_{D_{water}} A}}\,. \tag{75}$$

Now, taking the dimensional equation for Region 1 from the two-fluid model, and assuming

$C_D$ in air to be zero, we have

$$mh_1^{''} = (\rho_m - \rho_1)Vg\,, \tag{76a}$$

$$h_1(0) = 0\,, \tag{76b}$$

$$h_1^{'}(0) = 0\,. \tag{76c}$$

Integrating, we find

$$h^{'} = \frac{(\rho_m - \rho_1)Vg}{m}t\,, \tag{77a}$$

$$h = \frac{(\rho_m - \rho_1)Vg}{m}t^2\,. \tag{77b}$$

Setting $h^{'} = v_t$, we solve for $t$ and use it to determine $h$. This is the height above the interface at which we drop the sphere in order to achieve the fastest drop time.

# Experiment

## Two-fluid experiment

The two-fluid experiment is set up as follows. (We will not discuss the one-fluid experiment since that model is included in our two-fluid model). A large glass container is filled with the fluids being tested. The fluid combinations we tested were oil and water, and air and water. Figure 3 shows the experimental set-up for the air and water experiment.

In order to collect data, we obtained images of the experiment using high-speed photography. The high-speed digital camera used in this experiment is the Fastcam-512 PCI from Photron. It has a resolution of up to $512 \times 512$ pixels and can record at speeds of up to 32,000 fps. It operates directly from the computer using the software that was included with the camera. The camera is set up level with the glass container.

The ball is held in Fluid 1 at the total drop height $L_{tot}$. The ball is then dropped, and its motion from Fluid 1 into Fluid 2, and then through Fluid 2 is recorded using the high-speed

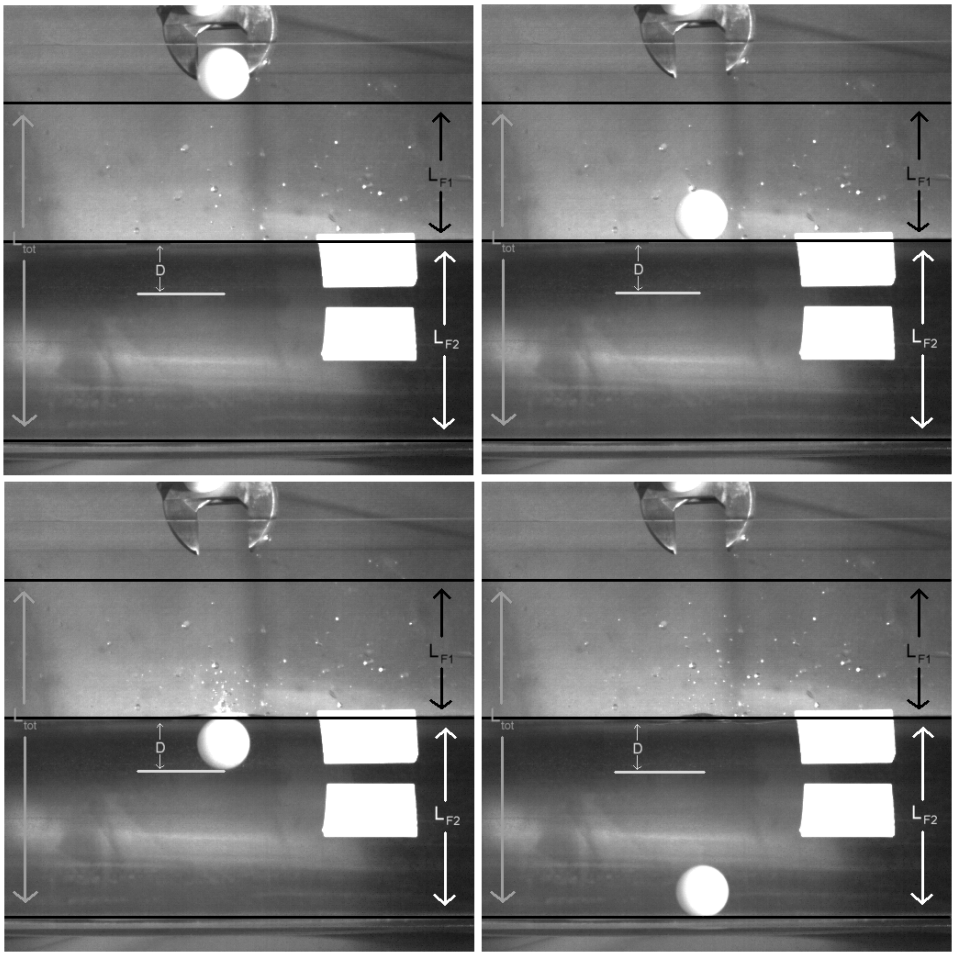


Figure 3: Still images of motion of a ball through air and water.

camera.

We used three different spheres for all of our experiments. (Note: using a ball that is much smaller than the container allows us to neglect the effects of the sides of the container on the motion of the ball for this section of the experiment.) Table 1 summarizes the measurements for Sphere 1, Sphere 2, and Sphere 3.

The densities of air, water, and oil are $1.29$ kg/m$^3$, $998$ kg/m$^3$, and $925$ kg/m$^3$ respectively.

For both two-fluid experiments, the data was taken from the high-speed video of the motion

| measurement | Sphere 1 | Sphere 2 | Sphere 3 |
|---|---|---|---|
| radius $r$ | $0.00954$ m | $0.0127$ m | $0.0063$ m |
| mass $m$ | $0.0041$ kg | $0.0096$ kg | $0.0012$ kg |
| density $\rho_m$ | $1141.6$ kg/m$^3$ | $1118.0$ kg/m$^3$ | $1145.7$ kg/m$^3$ |
| volume $V$ | $3.5914 \times 10^{-6}$ m$^3$ | $8.5800 \times 10^{-6}$ m$^3$ | $1.0500 \times 10^{-6}$ m$^3$ |

Table 1: Measurements for Sphere 1, Sphere 2, and Sphere 3.

of the ball. We extracted four still photographs of the motion before the ball is dropped, right before it begins to enter the second fluid, right as it leaves the first fluid, and finally when it hits the bottom of the container (Figure 3). Each image was analyzed in MATLAB in order to find the height in pixels at each frame. The height was measured from the bottom of the ball. Using the length scale found from the videos, we converted from pixels to meters and used the times of each frame to obtain the time in seconds. The coordinate system we used to make this conversion has its origin at the drop height of the ball, and the height is considered to be the distance from the drop height. This information gives us times to fall through the length of Fluid 1 $L_{F1}$, the transition zone $L_{trans} = 2r$, $r$ being the radius of the ball, and then the length of Fluid 2 $L_{F2} - 2r$. These times can be added together to obtain the total drop time.

We used Sphere 2 for the water and oil experiment. Table 2 summarizes the results of the experiment.

| time (sec) | height (m) |
|---|---|
| 0.000 | 0.000 |
| 0.407 | 0.042 |
| 0.532 | 0.068 |
| 0.821 | 0.123 |

Table 2: Results from water and air experiment.

For the water and air experiment, we used Sphere 1. Table 3 summarize the results.

| time (sec) | height (m) |
|---|---|
| 0.000 | 0.000 |
| 0.125 | 0.079 |
| 0.143 | 0.100 |
| 0.265 | 0.182 |

Table 3: Results from water and air experiment.

## Wall effect experiment

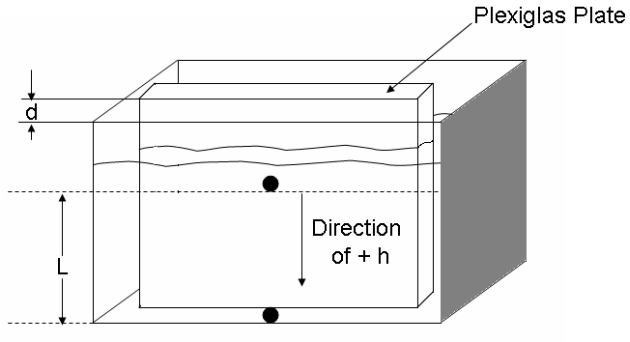


Figure 4: Set-up of wall effect experiment.

This experiment uses a rectangular tank filled with water, with a plexiglass plate inserted into the tank at a distance $d$ away from the front wall of the tank (Figure 4). The distance $d$ is manipulated so that the ratio of the radius of the sphere to its distance from the walls is less than $0.15$. The density of water is $\rho_l = 998$ kg/m$^3$ at $20^\circ$ C.

We used Sphere 2 for Trial 1 of the experiment. The plate was set up so that the radius of the confined space was $R = 0.0936$ m, giving us a sphere to container ratio of $0.14$. For Trial 2, we used Sphere 3, and the radius of the confined space was $R = 0.045$ m. Table 4 shows the results of this experiment.

| | Trial 1 | Trial 2 |
|---|---|---|
| height | $0.085$ m | $0.083$ m |
| time | $0.502$ s | $0.588$ s |

Table 4: Results from wall effect experiment.

### Optimization experiment

The goal of this experiment was to find the drop height that allowed the ball to have the fastest fall time in the two-fluid set-up. The two fluids used in this experiment were air and water, and the sphere used was Sphere 1. We dropped the ball from between $0.005$ m and $0.040$ m above the interface, in $0.005$ m increments. We performed three trials for each drop height, and averaged the results. Table 5 summarizes the results of this experiment.

| drop height above interface (m) | time to fall (sec) |
|---|---|
| 0.005 | 0.247 |
| 0.010 | 0.232 |
| 0.015 | 0.228 |
| 0.020 | 0.223 |
| 0.025 | 0.222 |
| 0.030 | 0.216 |
| 0.035 | 0.221 |
| 0.040 | 0.221 |

Table 5: Results from optimization experiment.

## Comparison of Theory and Experiment

### Two-fluid comparison

For both two-fluid experiments, we used the experimental data to solve our nondimensionalized equations from our model. We nondimensionalized our data and plugged it into Equations (57a-60f).

From our nondimensionalized data for the water and oil experiment, for Region 1, the $T_1$ we used was $1.5096$, which was the time of the fall through Fluid 1. The ODE was solved numerically over the interval $T = [0, 1.5096]$. Our goal was to find $\varepsilon$ such that $H(T_1) = 0.3415$. This was found through the bisection method to be $\varepsilon = 15.209765625$ (a tolerance of $10^{-6}$ was used). We used this experimentally obtained value of $\varepsilon$ in order to solve for $C_{D_1}$. We used the solution to the ODE for Region 1 in order to obtain initial condition (58c) for Region 2. The ODE for Region 2 was then solved numerically over the interval $T = [1.5096, 1.9733]$. Again, we found initial condition (59c) using the solution for Region 2. We used the coefficient of drag for water obtained from a previous experiment for $C_{D_2}$. Finally, we numerically solved the ODE for Region 3 over the interval $T = [1.9733, 3.0453]$. From our solution, we found $H_3(T_3) = 0.99109$, which is only a $0.891\%$ error from the expected value of $1$.

We used the same process for the water and air experiment with one minor change. Instead of having to find $\varepsilon$ and thereby finding $C_{D_1}$, we assumed that the coefficient of drag in air is negligible, and took $\varepsilon = 0$. Following the same procedure as before, we found $H_3(T_3) = 0.9060$, which is only a $9.4\%$ error from the expected value of $1$.

To compare our two-fluid model even further, we look toward the results of Competition 3. For this competition, we were given a height at which to drop a sphere of a specified size from air into water. We were asked to predict the fall time of the sphere through both fluids. This prediction was then compared to experimental data obtained.

The sphere that we used for this competition has a radius $r = .01908$ m, and the heights specified were $L_{F1} = 0.05$ m and $L_{F2} = 0.09$ m. Using our model for the two fluids, we made a fall time prediction of $t_f = 0.2289$ s. After three trials, we calculated the average fall time to be $t_f = 0.234$ s. This is a percent error of $2.18\%$, showing that our model is fairly accurate.

## Wall effect comparison

Using the experimental data from Trials 1 and 2, we solved our nondimensional equations to predict the fall time for each ball at their drop heights. We nondimensionalized our data and plugged it into our one-fluid model. The correction factor $K_w$ that we calculated for both trials is $1.162$. This $K_w$ is multiplied onto Equation 36, the original formula for $\varepsilon$ from the one-fluid model.

For Trial 1, we calculated $\varepsilon = 2.26303$ and $\tau = 0.2816$ using data from the experiment. We numerically solved the ODE for this trial and found the nondimensional fall time to be $T = 1.9632$. Scaling back to seconds, we have the fall time $t = 0.553$ s. This is only a $9.2\%$ error from the experimentally found value of $t = 0.502$ s.

For Trial 2, we calculated $\varepsilon = 4.43709$ and $\tau = 0.255865$. Again, we numerically solved the ODE, yielding a nondimensional time $T = 2.4354$. Scaling back, the dimensional fall time is $t = 0.623$ s. This is only a $5.6\%$ error from the experimentally found value of $t = 0.588$ s.

## Optimization comparison

Using the theory discussed in the optimization section, we calculated the terminal velocity and found the optimal drop height using Sphere 1. The calculated terminal velocity was $v_t = 0.2273$ m/s. Solving for $t$ and plugging this into the equation for the optimal height yields $h_{optimal} = 0.005$ m.

In our experiment, we tested drop heights between $0.005$ m and $0.040$ m. Our experimental results suggested that $0.030$ m was close to the optimal height. Our theoretical $h_{optimal}$ does not correlate well with this, but the theory predicts the optimal drop height for a perfect drop of the sphere. In order to obtain more accurate results, it may be necessary to use a more repeatable test set-up to ensure that the ball drops perfectly straight and at the exact drop height desired.

# Conclusion

Through the last three months, we have become much more aware of the various forces that act on a falling sphere through various fluids. Using these forces, we were able to produce mathematical models that can be used to predict the falling of these spheres given various properties of the sphere and fluids. Using these models, we successfully completed a number of competitions including fall time through one fluid, fall time through two fluids, optimized fall time through two fluids, and the effects that the container/sphere geometry have on the fall time of a sphere. We were able to make these predictions and verify them using experiments with little error. These competitions helped to prove that the models that we have developed are accurate at predicting the fall times of spheres through fluids.

# Appendix A

In this appendix, we have the MATLAB code that was used to numerically solve the ODEs in our models. Figures 5, 6, and 7 correspond to the three ODEs in our two-fluid model. We fill in the calculated values of $\varepsilon$, $D$, $L_{tot}$, $L_{F_1}$, $\delta$, $\beta$, and $\gamma$ where there are blanks in the code. Figure 8 shows an example of the code used to solve one of the ODEs.

```
function yprime = m3odesysl(t,y)
% Second order differential equations made into
% system of first order equations

E= ;            %epsilon
yprime = zeros(size(y));
yprime(1) = y(2);
yprime(2) = -E*y(2)^2 + 1;
yprime(3) = y(4);
yprime(4) = -y(2)^2 - 2*E*y(2)*y(4);
```

Figure 5: MATLAB code for ODE for Region 1.

```
function yprime = m3odesys2(t,y)
% Second order differential equations made into
% system of first order equations

D = ;           %diameter of sphere
Lt = ;          %Ltot
Lf = ;          %Lfl
E = ;           %epsilon
d = ;           %delta
B = ;           %beta
C = sqrt(D^2 - (D - Lt*y(1) - Lf)^2)/Lt;
G = -(y(1) - Lf/Lt - D/Lt)/sqrt((2*D*(y(1)-Lf/Lt))/(Lt^2) - (y(1) - Lf/Lt)^2);

yprime = zeros(size(y));
yprime(1) = y(2);
yprime(2) = (d + (E - B*C^2*G)*y(2)^2)/(B*C^3 +1);
```

Figure 6: MATLAB code for ODE for Region 2.

```
function yprime = m3odesys3(t,y)
% Second order differential equations made into
% system of first order equations

E= ;            %epsilon
g = ;           %gamma
d = ;           %delta
yprime = zeros(size(y));
yprime(1) = y(2);
yprime(2) = -E*g*y(2)^2 + d;
```

Figure 7: MATLAB code for ODE for Region 3.

```
[t,y] = ode45('m3odesys1',[0,2],[0,0,0,0]);

plot(t,y(:,1))
title('Solution of ODE, height vs. time (nondimensional)')
xlabel('time T')
ylabel('height H')

[t,y(:,1)]
```

Figure 8: MATLAB code to solve ODE.

# References


1. N. Abaid, D. Adalsteinsson, et al., *An internal splash: levitation of falling spheres in stratified fluids*, Physics of Fluids, 16, (2004), pp. 1567-1580.

2. E.G. Richardson, *The impact of a solid on a liquid surface*, Proc. of the Phys. Soc., 61, (1948), pp. 352-367.

3. K. Renganathan, R. Turton, and N.N. Clark, *Accelerating Motion of Geometric and Spherical Particles in a Fluid*, Powder Technology, 58, (1989), pp. 279-284.

4. R. Turton and O. Levenspiel, Powder Technology, 47, (1986).

5. F.M. White, Fluid Mechanics, McGraw-Hill Higher Education, (2003).

6. M. Jenny and J. Dusek, *Efficient numerical method for the direct numerical simulation of the flow past a single light moving spherical body in transitional regimes.*, J. Comput. Phys., 194, (2004), pp. 215-232.

7. M. Jenny, J. Dusek, and G. Bouchet, *Instabilities and transition of a sphere falling or ascending freely in a Newtonian fluid.*, J. Fluid Mech., 508, (2004), pp. 201-239.

8. E.T.G. Bot, M.A. Hulsen and B.H.A.A. van den Brule, *The motion of two spheres falling along their line of centres in a Boger Fluid*, J. Non-Newtonian Fluid Mech., 79, (1998), pp. 191-212.

9. Binhua Lin, Jonathan Yu, and Stuart A. Rice, *Direct measurements of constrained Brownian motion of an isolated sphere between two walls*, Physical Review E, 62, (2000).

10. P.Y. Huang and J. Feng, *Wall effects on the flow of viscoelastic fluids around a circular cylinder*, J. Non-Newtonian Fluid Mech., 60, (1995), pp. 179-198.